Published in final edited form as:
Traffic. 2011 February ; 12(2): 170–184. doi:10.1111/j.1600-0854.2010.01145.x.

The role of ubiquitination in lysosomal trafficking of δ-opioid receptors

Anastasia G Henry[1], **Ian J. White**[4], **Mark Marsh**[4], **Mark von Zastrow**[1,2,3], and **James N Hislop**[2,3]

[1] Program in Cell Biology, University of California, San Francisco

[2] Department of Psychiatry and Cellular, University of California, San Francisco

[3] Department of Molecular Pharmacology, University of California, San Francisco

[4] Cell Biology Unit, MRC Laboratory for Molecular Cell Biology and Department of Cell and Developmental Biology, University College London

Abstract

Lysyl-ubiquitination of signaling receptors is widely recognized to drive their proteolytic down-regulation via the multivesicular body (MVB) / lysosome pathway. Ubiquitination can act at multiple steps in this pathway, depending on receptor type and organism examined. No previous study has identified specific trafficking step(s) controlled by ubiquitination of a mammalian seven-transmembrane receptor (7TMR). The δ-opioid receptor (DOR) undergoes ligand-induced is a mammalian 7TMR down-regulation by ESCRT-dependent endocytic trafficking to lysosomes. In contrast to a number of other signaling receptors, the DOR can down-regulate effectively when its ubiquitination is prevented. We explored the membrane trafficking basis of this behavior. First, we show that that undergoes rapid lysosomal down-regulation physiologically, but this 7TMR has a still-unexplained ability to down-regulate effectively even when its ubiquitination is blocked. define pathway underlying internalized DORs traverse the canonical MVB pathway and localize to intralumenal vesicles (ILVs). Second, we show that DOR ubiquitination stimulates, but is not essential for, receptor transfer to ILVs and proteolysis of the receptor endodomain. Third, we show that receptor uHere we show that DORs traffic via morphologically typical MVBs and, similar to other signaling receptors, ubiquitination of DORs promotes the transfer of receptors from the limiting membrane of MVBs into intralumenal vesicles (ILVs). However, biquitination plays no detectable role in the early sorting of internalized DORs out of the recycling pathway. Finally, we show that DORs undergo extensive proteolytic fragmentation in the ectodomain, even when receptor ubiquitination is prevented or ILV formation itself is blocked. Together these results are sufficient to explain why DORs down-regulate effectively in the absence of ubiquitination, and they place a discrete molecular sorting operation in the MVB pathway effectively upstream of the ESCRT. selectively of without More generally, these findings support the hypothesis that unlike other signaling receptors presently described, this topological sorting function is regulatory rather than essential. Further, ubiquitination of DORs plays no detectable role in excluding internalized receptors from the bulk-recycling pathway. Together, these observations are sufficient to explain biochemical data indicating that ubiquitination of DORs produces a relatively subtle effect on the later digestion of receptor-derived proteolytic fragments. To our knowledge, this study provides the first systematic analysis of the role of ubiquitination in mediating lysosomal down-regulation of a mammalian 7TMR. This sbiochemically and

Correspondence: Mark von Zastrow, N212E Genentech Hall, UCSF Mission Bay Campus, 600 16th St, San Francisco, CA 94158-2140, phone 415-476-7855; fax 415-514-0169; mark.vonzastrow@ucsf.edu.

functionally distinct mammalian cells can control the cytoplasmic accessibility of internalized signaling receptors independently from their ultimate trafficking fate.

Keywords

GPCR; microscopy; sorting; ubiquitin

Introduction

Endocytosis represents perhaps the most highly conserved mechanism by which cells control receptor-mediated signaling processes (1,2). The importance of endocytic regulation is clearly evident for seven-transmembrane receptors (7TMRs), the largest family of signaling receptors expressed in animals. Endocytosis of 7TMRs can mediate diverse functional effects, which depend largely on the subsequent trafficking itinerary of particular internalized receptors after endocytosis. Recycling of internalized receptors to the plasma membrane typically can promotes rapid recovery (resensitization) of cellular responsiveness in the face of repeated stimulation (3–5). In contrast, Rreceptor trafficking to lysosomes, in contrast, results in proteolytic down-regulation of receptors that and typically attenuatess cellular signaling responsiveness (6). Given these effectively opposite functional consequences, a critical question in the field is how receptor-specific differences in post-the endocytic trafficking trafficking of receptors are determined.

Lysyl-ubiquitination has emerged as a fundamental biochemical determinant of directing the endocytic trafficking of signaling receptors, as well as various and other membrane cargo, to lysosomes (6–10). Ubiquitination can affect endocytic trafficking at multiple steps, and the precise function(s) of ubiquitination differ depending on the receptor type and organism examined. Ubiquitination of yeast 7TMRs has been shown to promote endocytosis of receptors, prevent internalized receptors from entering the 'bulk flow' recycling pathway to the plasma membrane, and promote accelerate proteolytic destruction of internalized receptors by driving their transfer of receptors from the limiting endosome membrane to intralumental vesicles (ILVs). Ubiquitination of the mammalian EGF receptor tyrosine kinase in mammalian cells is not required essential for regulated endocytosis, but functions both to prevent recycling by the bulk pathway and to promote receptor accelerate proteolysis via receptor transfer to ILVs (11–15). Ubiquitination is thought to function similarly in Ubiquitination promoting lysosomal down-regulation of a number of mammalian 7TMRs of mammalian 7TMRs is also known to promote their down-regulation in the lysosome pathway, and appears to function largely downstream of endocytosis (*e.g.*, (6,16,17)). To our knowledge, however, no previous study has defined particular . However, it remains unknown precisely what step(s) in the in the down-regulation pathway that post-endocytic trafficking are regulated by ubiquitination of a pathway are affected 7TMR by ubiquitination of mammalian 7TMRs in mammalian cells..

The δ-opioid neuropeptide receptor (DOR) is a mammalian 7TMR that undergoes efficient lysosomal down-regulation via endocytic trafficking to lysosomes, both in cultured cell models and under physiological conditions in native tissues (18–21). Down-regulation of the DORs is particularly interesting because this process ESCRT-dependent, but DORs can have the remarkable ability to down-regulate occur efficiently effectively when receptor ubiquitination is prevented by mutation of all cytoplasmic lysine residues, yet requires ESCRT components when their direct ubiquitination is prevented by mutation of cytoplasmic lysine residues (22–24). Previous studies have identified additional proteins affecting dDown-regulation of the DORs is modulated by receptor interaction with additional cytoplasmic proteins, which are , distinct from the the conserved ESCRT and not

conserved in yeast machinery (25,26) but may interact with the ESCRT indirectly, which can mediate alternate connectivity to ESCRT 0 (27). Nevertheless, . Nevertheless, it is clear the wild type DOR s are is subject to extensively ubiquitinationed in intact cells, and DOR ubiquitination has been shown to function in ER-associated degradation (ERAD) of recently synthesized receptors by proteasomes (28,29). What significance, if any, direct ubiquitination plays in membrane trafficking event(s) mediating lysosomal down-regulation of the DOR has remained an unresolved issue.

Until recently, we were unable to discern any significant role of DOR ubiquitination in proteolytic down-regulation of receptors by endocytic trafficking to lysosomes. Positive The first evidence that for any effect of DOR DOR ubiquitination affects on lysosomal trafficking the down-regulation pathway emerged from a functional screen identifying a role of investigating the effects of a panel the HECT domain ubiquitin ligase AIP4 in modulating the kinetics of DOR down-regulation assessed by radioligand binding of candidate ubiquitin ligases on agonist-induced down-regulation of wild type DORs (24). This screen identified a specific role of the HECT domain E3 ligase AIP4, AIP4-dependent ubiquitination of a distinct 7TMR, the the same ligase shown previously to mediate 'direct' sorting of CXCR4 chemokine receptor, was shown previouslys to to function as a direct sorting determinant directing internalized receptors out of the recycling pathway and promoting their delivery to lysosomes (30). However, two observations argued against the this canonical sorting model in the case of DORs. First, while inactivation or depletion of AIP4 inhibited down-regulation only of wild type DORs while, in the same experiment, s, down-regulation of lysine-mutant DORs occurred with nearly wild type kineticsdown-regulated with nearly wild-type efficiency. Second, preventing DOR ubiquitination produced a relatively subtle effect on net down-regulation, which was detectable only after destruction of a substantial fraction radioligand binding sites had already occurred primarily affected DOR down-regulation at a relatively late stage in an extended process of receptor destruction, and was not required for the initial proteolytic fragmentation of receptors (24). It was therefore proposed that ubiquitination of the DOR mediates a regulatory, rather than essential, role in directing lysosomal destruction of this 7TMR. The nature of this proposed regulatory function has not been defined, nor has there been any progress in determining the membrane trafficking basis underlying the ability of ubiquitination-defective receptors to undergo effective ESCRT-dependent down-regulation.

The above observations We addressed these questions in the present study do not provide a clear picture of the role of ubiquitination in the membrane pathway mediating DOR down-regulation. Here we address this fundamental issue using a combination of biochemical, morphological and live imaging approaches. Our results establish that both wild type and lysine mutant DORs traverse traffic to lysosomes via the canonical MVB spathway, that , define a precise functional role of AIP4-dependent ubiquitination of DORs promotes but is not essential for receptor localization to ILVs, and that the previously identified alternate sorting mechanism functions upstream of the ESCRT in a sequential pathway of molecular sorting operations driving receptor trafficking to lysosomes. These results resolve a specific function of ubiquitination in ligand-induced down-regulation of the DOR, and suggest a means by which mammalian cells can in this pathway, and explain why ubiquitination of DORs has regulate the cytoplasmic accessibility of internalized signaling receptors independently from ultimate trafficking fate. only a modest effect on net receptor destruction.

Results

Lysine Ubiquitination is not required for efficient sorting of the DOR out of the rapid recycling pathway mutation does not cause enhanced recycling of DORs to the plasma membrane

We investigated the post-endocytic sorting of both the wild type DOR and a previously described mutant, DOR-0cK, which is devoid of all cytoplasmic lysine residues and is not ubiquitinated in intact cells (22–24). We added distinct N-terminal (FLAG) and C-terminal (HA) epitope tags to facilitate selective immunochemical detection of the receptor ectodomain and endodomain (F-DOR-HA and F-DOR-0cK-HA, Fig 1A), and expressed the tagged constructs in stably transfected HEK293 cells at moderate levels (~1 pmol / mg, see *Materials and Methods*) that have been shown do not to saturate the endocytic pathway (24).

We first asked if the lysine mutation caused increased recycling of DORs after agonist-induced endocytosis. We did so because a hallmark of ubiquitin-directed sorting of other signaling receptors in both yeast (31) and mammalian cells (14,17) is that lysyl mutation effectively redirects internalized receptors into the rapid recycling pathway. We measured DOR recycling using a previously described flow cytometric assay that monitors surface return of antibody-labeled receptors from the internalized pool (18,32). Both F-DOR-HA and F-DOR-0cK-HA internalized robustly in response to activation by the opioid peptide agonist 2-D-Ala, 5-D-Leu-enkephalin (DADLE), consistent with previous evidence that ubiquitination is not required for DOR endocytosis (22). Further, and also as shown previously (18), the vast majority of F-DOR-HA was retained in the endocytic pathway at all time points tested after removal of agonist from the culture medium (Fig .1B, filled squares). Importantly, and not previously established, the lysine-mutant F-DOR-0cK-HA receptor construct was retained in the endocytic pathway with indistinguishable efficiency relative to the 'wild type' F-DOR-HA (Fig .1B, open squares). Other mammalian 7TMRs, such as the β_2-adrenergic receptor, largely recycle return to the plasma membrane efficiently in this assay within <≤30 min after agonist washout (18). We also also verified, in parallel samples, nearly complete recycling return of internalized transferrin receptors (TfRs; Fig 1B, filled circles), that mark the rapid which are known to access the rapid recycling pathway (33), in parallel samples (Fig.1B, filled circles). Moreover we verified visually obvious retention in the endocytic pathway of both F-DOR-HA and F-DOR-0cK-HA after agonist washout by fluorescence microscopy using either epitope tag (Supplemental Fig.1).

Both wild type and lysine-mutant DORs localize to MVBs

Having established that lysine mutation of DORs is not required to prevent receptors from recycling to the plasma membrane, we next asked if internalized receptors traverse MVBs. While a number of 7TMRs have been shown to localize to MVBs, and to be capable of accessing intralumenal membranes in mammalian cells (34-37), this has not been investigated previously for opioid receptors. Moreover, to our knowledge, no previous study has specifically determined the whether ubiquitination-dependence is essential for intralumenal localization of any 7TMR in mammalian cells. We initially addressed these questions using immunogold labeling of cryosections followed by electron microscopy, allowing an established method allowing unambiguous resolution of precise resolution of intralumenal membranes. We examined receptor localization in cells fixed 90 min after DADLE application, a time point chosen because it is clearly after receptor sorting out of the recycling pathway (Fig 1B), and around the time that onset of substantial proteolysis of the DOR proteolysis is beginning to occur (see below). We localized anti-HA immunoreactivity because, irrespective of the degree of proteolytic fragmentation of receptors occurring at this time point,

Although iectodomain cleavage (see below) could potentially cause aberrant accumulation of the FLAG epitope in MVBs, intralumenal accumulation localization of ththee C-terminal HA epitope is topologically impossible unless physical transfer to ILVs has occurred. We therefore focused in these studies on localization using anti-HA.

In cells expressing 'wild type' F-DOR-HA, aAnti-HA immunoreactivity representing wild type DOR localized robustly to MVBs, and could be clearly resolved in association with both the limiting and intralumenal membranes (Fig 1C). Anti-HA iImmunoreactivity representing in cells expressing the lysine-mutant DOR-0cK also localized to MVBs at this time point and, remarkably, was observed both in association with both the limiting and intralumenal membranes (Fig 1D). Examination across numerous sections verified these findings, establishing definitively the ability of both wild type and lysine-mutant receptors to localize to MVBs and gain intralumenal access. We noted, however, considerable variability across individual MVBs in the apparent degree of to which immunoreacitivty accessed intralumenal membranes localization (randomly selected examples for each receptor construct are shown in Supplemental Fig 2). This motivated us to verify, and further investigate, intralumenal localization . of receptors using methods that are more amenable to global analysis across a larger representation of the cell population.

We next asked if we could observe intralumenal distribution of receptors by fluorescence microscopy. Accordingly As a first step to do so, we replaced the C-terminal HA tag with GFP (F-DOR-GFP and F-DOR-0cK-GFP). We verified biochemically that the GFP tag did not compromise agonist-induced down-regulation (Supplemental Figure 3), and then expressed a mutationally constitutively-activatede mutant form of Rab5 (CFP-Rab5Q79L) to enlarge endosomes and facilitate optical resolution of limiting and intralumenal membranes (35, 38). As observed with electron microscopy, confocal fluorescence microscopy verified that both GFP-tagged wild type and lysine-mutant receptor variants localized both peripherally and intralumenally in endosomes. Also consistent with the electron microscopic observations, we observed considerable variability in localization across individual endosomes, including among those imaged within the same cell (Fig. 2A and B**, see ***).

Although it is cHaving established lear that both the both DOR and DOR-0cK are both able to access ILVs, we next next used this approach to asked whether if lysine mutation affects the degree to which tagged receptors localize to the endosome lumen. To quantify the extent of intralumenal distribution, we used line scan analysis of confocal cross-sections (Fig. 2C) and carried out this analysis over a large number of examples selected at random from multiple cells and experiments. This analysis revealed a partial but significant reduction in the relative amount of lysine-mutant receptors present in the endosome lumen compared to that observed for wild type receptors (Fig 2D).

While cCo-expression of activated Rab5 has was been required essential to reliably achieve optical resolution of resolve the intralumenal space of endosomes in fixed specimens., Rwe were surprised to observe that receptor-containing endosomes were significantly larger in living cells (typically 1 – 2 μm diameter), however, making it was possible to resolve the lumen were considerably larger in living cells (typically 1 – 2 μm) than by spinning disc confocal microscopy in the absence of mutant Rab5 previously observed in fixed specimens (<500nm). This allowed us to achieve optical resolution of the lumen even in the absence of mutationally-activated Rab5. SimilarA similar line scan analysis verified a partial but significant reduction of intralumenal receptor fluorescence produced by lysyl mutation under these conditions (Fig 3A–C, Supplemental Mmovie 1 and 2). We also observed that intralumenal localization of both receptor variants was inhibited in cells exposed to the PI3 kinase inhibitor wortmannin, and by in cells over-expressingon the ESCRT-0 component of the ESCRT-0 component HRS (Fig 3D -I). Both of these manipulations have been used

previously to define the ESCRT-dependent mechanism of ILV formation relative to alternate ESCRT-independent mechanism(s) (39,40). Thus, the present results suggest that both wild type and lysine-mutant DORs can access the intralumenal space of MVBs, apparently do so via primarily by the canonical (canonical, ESCRT and PI3K -dependent) mechanism, and ubiquitination o.f the DOR stimulates but is not required for this topological sorting operation.

While our localization data clearly established receptor intralumenal localization of both wild type and lysine-mutant DORsin the endosome lumen, they did not provide information about whether this topological sorting is sufficient to expose topological redistribution of receptors results in exposure of the receptor endodomain to the biochemical environment of the endosome lumen. As a first step to address this question, we replaced the C-terminal (endodomain) tag with a GFP variant, ecliptic pHluorin (41), whose fluorescence is efficiently and reversibly quenched when exposed to the acidic environment of the endosome lumen (Fig 4A).

Using this approach, we were able to selectively visualize tagged receptors localized in the limiting membrane and then, in a time-dependent manner after the addition to cells of the membrane-permeant weak base chloroquine, neutralize the endosome interior and reveal the presence of any tagged receptors present in the endosome lumen (and which were previously undetectable due to fluorescence quenching). This approach definitively confirmed the presence of intralumenal receptors (Fig 4B and C, Supplemental Mmovie 3 and 4), and at the same time point as used for the other analyses. Quantification of the chloroquine-induced increase in fluorescence intensity confirmed partial inhibition of intralumenal localization produced by lysyl mutation (Fig 4D). These results, in addition to definitively verifying intralumenal localization of receptors at the light microscopic level, indicated that intralumenal receptors indeed gain biochemical access to the acidic environment of the endosome endocytic pathwaylumen.

Lysine mutation of DORs delays proteolytic destruction specifically of the receptor endodomain

We next asked if how this this regulatory, but non-essential, function of apparent function of DOR ubiquitination affects the process of receptor degradation in the endocytic pathway. in promoting endodomain access to the lumenal environment produces a functionally relevant effect on DOR proteolysis. To do so we used the dual epitope tagging strategy (Fig 5A) to monitor proteolysis in the receptor ectodomain (N-terminal FLAG tag) compared separately from the to endodomain (C-terminal HA tag).

Consistent with previous studies examining proteolysis of the DOR N-terminus (22,23), immunoblotting using anti-FLAG antibody verified proteolysis of the FLAG tag from F-DOR-HA that began ~60 min after agonist addition was essentially complete within 2 hours thereafter (Fig 5B). The rate and extent of this proteolysis were completely unaffected by lysine mutation (Fig 5C), as verified by densitometric quantification across multiple experiments (Fig 5D). Immunoblotting of the same extracts using anti-HA verified extensive proteolytic fragmentation of both F-DOR-HA and F-DOR-0cK-HA in DADLE-exposed cells (Fig 5E and F). The onset of this fragmentation corresponded closely precisely to with loss of the ectodomain FLAG epitope. Interestingly, while essentially no full-length forms of either receptor construct (indicated by bracket) remained after ~3 hours of DADLE exposure, we noticed a relative the accumulation of HA-linked proteolytic fragments at later time points preferentially in cells expressing lysine-mutant receptors (arrows at right of the blot). Quantification across multiple experiments verified a significant difference in the persistence of intermediate HA-linked fragments between wild type and ubiquitination-defective mutant receptors (Fig 5G).

These observations support the hypothesis that DOR ubiquitination selectively promotes destruction of the DOR endodomain, consistent with enhanced biochemical access afforded by intralumenal transfer.

We To further further investigate the biochemical consequence of preventing DOR ubiquitination,d this hypothesis by more detailed analysis of the proteolytic fragmentation of lysine-mutant DORs. To accomplish this we immunoprecipitated HA-linked fragments, removed Asn-linked glycans with PNGaseF, and estimated the molecular mass of each fragment by calibrated SDS-PAGE. Full-length DORs resolved at ~453 kDa after deglycosylation, as expected for the doubly tagged protein (predicted 42.6 kDa with epitope tags). In the presence of DADLE, we observed time-dependent formation of Agonist treatment revealed additional proteolytic fragments resolvinged at 38, 31 and 22 kDa (Fig 6A). Mapping these fragments . All of these products mapped to cleavages occurring in to the predicted topology of the full-length, tagged receptor unambiguously established that each of the observed fragments resulted from proteolysis specifically in the receptor the ectodomain (Fig 6B). These results further . These results ssupport the hypothesis that DOR ubiquitination selectively promotes proteolysis of the receptor endodomain. They also and indicate that, when DOR ubiquitination is prevented by lysine mutation, receptors can still undergo extensive proteolytic fragmentation at multiple sites distributed throughout the ectodomain.

B

As an independent approach to investigate if this selective effect on endodomain proteolysis is a consequence of sorting of receptors to the MVB lumen, we next asked if pharmacological blockade of net MVB formation by using the PI3K inhibitor wortmannin (42) producehad s little a similar effect on wild type receptors. Wortmannin had little effect on DADLE-induced destruction of the luminal FLAG epitope (Fig 7A and B), but caused resulted in a pronounced accumulation of HA-linked proteolytic fragments similar to those accumulated by preventing receptor ubiquitination (Fig 7 C and D). This result further further indicates that supports the importance of ubiquitin-promoted intra-MVB sorting of DORs in selectively enhancing promotes proteolytic destruction of the receptor DOR endodomain, but not for without affecting the ability of receptors to undergo extensive fragmentation proteolytic cleavage of the receptor by proteolysis in the ectodomain.

Disrupting AIP4 activity phenocopies the lysine-dependent trafficking effect on wild type DORs

Having established a specific effect of lysine mutation on both intra-MVB sorting and endodomain proteolysis of DORWs, we next took asked if this selective effect on endodomain proteolysis and intra-MVB sorting of the DOR is a consequence of ubiquitination mediated by AIP4. an independent approach to examine if these effects truly result from a lack of receptor ubiquitination or might reflect some other (ie pleiotropic) effect of mutating multiple lysine residues. To do so, we took advantage of the ability of applied a previously established dominant negative strategy using catalytically-inactivemutationally inactivated (Cys->Ala or C/A mutant) mutant version of the E3 ligase AIP4 to inhibit ubiquitination of the wild type DOR (24),), and asked if expression disrupting AIP4 activity can mimic of this construct phenocopied the lysine-mutant effects of lysine mutation in the context of the wild type DOR.

Using the dual epitope strategy, we observed that We examined the effect of co-expressing inactive AIP4 on DADLE-induced proteolysis of both FLAG (ectodomain) and HA (endodomain) epitopes fused to the wild type DOR. Consistent with the results from study of lysine-mutant DORs, disrupting AIP4 activity did not affect DADLE-induced proteolysis

of the wild type DOR ectodomain (Fig 8A) but significantly inhibited the subsequent destruction of endodomain-linked proteolytic fragments (Fig 8B).

Using the GFP imaging line scan analysis strategy, we then established that co-expression of a (Cherry-tagged) inactive AIP4 C/A mutant inhibited intralumenal localization of the wild type DORs fused in the endodomain (C-terminal tail) to GFP. In contrast, co-expression at similar levels (assessed by Cherry fluorescence) of an inactivated mutant form of Cherry-tagged version of the related HECT domain ligase, Nedd4-2,, which does not inhibit down-regulation of wild type DORs, had no effect (Fig 8C). Further In contrast, and verifying that the DOR is a direct target of AIP4-dependent ubiquitination, , as an additional control for specificity, we used the same method to verify that co-expression of Cherry-tagged C/A mutaninactivated t AIP4 did not affect produce any detectable effect on intralumenal localization of the lysine mutant DORs (Fig 8D). Together, these results recapitulate the specific trafficking and degradative effects of DOR lysine mutation, verifying that these effects indeed represent a specific consequence of DOR ubiquitination by AIP4.

Discussion

The presentse results provide a systematic analysis of the membrane trafficking events underlying lysosomal down-regulation of the DORs. We studied focused on this particular mammalian 7TMR because its lysosomal destruction is a physiologically important regulatory process (20,21), and because DORs have the the remarkable remarkable ability to down-regulate effectively via an ESCRT-dependent mechanism when their ubiquitination is prevented. Previous work identifying has described alternate (non-ESCRT) protein connectivity modulating DOR down-regulation influencing DOR trafficking after endocytosis (25,27) leaves unresolved whether DORs traverse MVBs and, if so, what role. Thus we focused on defining precisely what role ubiquitination plays in mediating or controlling the the endocytic membrane trafficking of down-regulation of this mammalian 7TMR, and determining how this trafficking function affects the process of receptor proteolysis..

Our data clearly establish that internalized DORs traffic via morphologically characteristic MVBs, and localize to the endosome lumen in an ESCRT and PI3K -dependent manner, which supporting the hypothesis that DORs traverse the canonical MVB pathway represent canonical intermediates in the pathway mediating down-regulation of diverse signaling receptors (43). Accordingly, we took several independent approaches to discern the specific functional significance of DOR ubiquitination to receptor trafficking within this pathway. First, we assessed the sorting of receptors away from bulk membrane recycling using an established flow cytometric method. Second, we investigated whether receptors traverse MVBs by using immunoelectron microscopy and using several optical imaging approaches. Third, we assessed examined the effect of intra-MVB sorting on biochemical accessibility of receptors to the endosome lumen using both pH-sensitive GFP (pHluorin) imaging and biochemical analysis of domain-specific proteolytic fragmentation.

Exclusion of DORs from bulk the rapid recycling pathway marked by TfRs was highly efficient, was was not detectably inhibited by lysine mutation of receptors, and clearly preceded the onset of proteolytic digestion of receptors measured by any of the biochemical assays. These findings define receptor sorting away from the bulk recycling route as a discrete, and early, sorting operation. Quantitative imaging revealed that uUbiquitination of DORs specifically promoted their later intralumenal localization to the intralumenal compartment of endosomes of internalized DORs. This is consistent with the ability of ubiquitination of various integral membrane proteins to promote intra-MVB sorting, of many integral membrane proteins with the two notable exceptions: First, that **1)**

ubiquitination of DORs was not essential for intralumenal localization, (as lysine-mutant receptors were clearly observed to access the endosome lumen both by immuno-electron microscopy and fluorescence imaging of living cells), and **2)** . Second, that neither DOR ubiquitination nor intra-MVB sorting was required to prevent internalized receptors from recycling to the plasma membrane.

Together, thesethese results observations support a model with in which endocytic trafficking of the DOR to lysosomes involves two discrete molecular sorting operations that are arranged in series in the MVB pathway, and which differing in dependence on receptor ubiquitination (Fig. 9). Importantly, the finding that lysyl mutation of DORs reduces intralumenal sorting of DORs localization without causing any enhancement of receptor recycling rules out the alternative hypothesis that ubiquitin -independent and -dependent mechanisms function in parallel.

T, and indicates tha the first operation is the the ubiquitin-dependent exclusion of internalized receptors from the rapid recycling pathway mechanism functions upstream. The first of these sequential sorting operations, effective exclusion of DORs from the bulk recycling pathway, is completely insensitive to receptor ubiquitination and is ('Sorting Step I' in Fig 9); this sorting step does not require ubiquitination of the DOR and, for this particular 7TMR, represents the major major determinant of subsequent the receptor’s ultimate endocytic trafficking fate. This is In contrast, remarkable because previous studies have shown that lysyl mutation has been shown to markedly increase s recycling of other several other signaling receptors in both yeast and mammalian cells (14,31), including some the other mammalian GPCRs PAR2 and NK1R7TMRs (17,44). This suggests that the upstream sorting step represents an elaboration of the down-regulation pathway that is engaged specifically by a subset of signaling receptors.

The second sorting operation in the serial sequential model is receptor ttransfer of DORs from the endosome limiting membrane to ILVs ('Sorting Step II' in Fig 9). This topological sorting operation is promoted stimulated by DOR ubiquitination, and is thus similar to corresponds to the primary sorting operation distinguishing recycling from degradative trafficking of various other signaling receptorsof 7TMRs in yeast and the EGF receptor in mammalian cells. A distinction is that, for the DOR, , relative to previously investigated signaling receptors, is that lysyl-ubiquitination promotes but is clearly not essential for topological sorting to receptor localization to ILVs. This verifies the dominant role of Sorting Step I in directing DOR trafficking to the MVB pathway, and suggests that this upstream sorting operation is sufficient to drive effective delivery of receptors to sites of ESCRT-mediated ILV formation even in the absence of receptor ubiquitination..

The Live imaging of pHluorin-tagged receptors data established indicate that intra-MVB sorting of DORs to the endosome lumen affords access of the receptor endodomain to the acidic environment of the endosome lumen. The proteolytic cleavage data analysis confirm showed, further, and extend this conclusion, a thats intra-MVB sorting selectively acceleratesd destruction of the receptor endodomain. Thus the present results can simply explain why previous studies of DOR ubiquitination have detected only a relatively subtle effect on net proteolytic destruction of DORs.

An important question for future study is how receptors devoid of any ubiquitination retain the ability to undergo sorting to undergo topological sorting to ILVs the MVB lumen. While wee note that there is considerable evidence for the existence of alternate mechanisms of intra-MVB trafficking ILV formation and cargo traffic (39,40). Our , our data results suggest strongly suggest that both wild type and lysine-mutant non-ubiquitinated DORs access the endosome lumen by the canonical (ESCRT-dependent) mechanism dependent on

ESCRT 0 and PI3K, rather than alternate mechanism(s) with different biochemical features (39,40). The simplest hypothesis capable of explaining the present findings is that The simplest possibility is that nonon-ubiquitinated receptors, because they are unable to efficiently enter the rapid recycling pathway originating from early / sorting endosomes, are effectively 'trapped' in maturing endosomes and subsequently access the intralumenal compartment during the process of MVB biogenesis simply by lateral passive diffusion into ESCRT domains in formed at the limiting membrane. An additional, and not mutually exclusive, possibility is that alternate DOR (i.e. not mediated by ubiquitin interaction) connectivity of DORs to the ESCRT 0 (25,27), as proposed here to function in Sorting Step I, persists during MVB biogenesis at later stages of endosome maturation and further to further facilitate promote ESCRT-mediated entry into the intralumenal compartment (Fig. 9, inset). Either or bBoth of these mechanisms are plausible based on present information, and could simply account for the ability of non-ubiquitinated DORs to undergo sorting to ILVs. Finally, wWe cannot exclude the possibilityy that topological DOR sorting of DORs trafficking to ILVss is promoted by interaction with a distinct, ubiquitinated linker protein or other receptor (and likely ubiquitinated) endocytic cargo protein, or that DORs access ILVs by lateral partitioning into biophysically distinct microdomains of the limiting membrane from which ESCRT-dependent ILV formation occurs. We note that, while that DORs DORs are known to have the ability to homo-oligomerize when present at high surface concentration, and may also and form hetero-oligomers specfically with other opioid receptor subtypes 7TMRs (45), HEK293 cells do not express any opioid receptors endogenously. Any of these possibilities could explain the ability of DORs to undergo topological sorting in the absence of ubiquitination, and none would Further, even if DOR sorting is assisted by association with an (as yet unknown) ubiquitinated intermediary of some kind, this possibility would not fundamentally alterinvalidate the present conclusion that DORs are sorted sequentially in the MVB pathway. the present interpretation that biochemically distinct sorting steps allow mammalian cells to selectively control the ultimate trafficking fate of DORs independently from topological sorting to ILVs.

Another interesting important question for future investigation is to determine the functional significance of what functional advantage is conferred by distributing the endocytic trafficking of DORs into discrete, and sequential molecular , sorting operations in the pathway of DOR down-regulation. An An obvious attractive possibility, as mentioned above, is that thiss equential sorting could organization could provide the cell wiafford an than additional degree of freedom in the endocytic regulation of particular signaling receptors, by effectively allowing to control the cytoplasmic accessibility of internalized internalized signaling receptors to be controlled specifically and independently from independently from their their ultimate trafficking fate. There is accumulating evidence that various signaling receptors, including some 7TMRs, can signal from endosomes as well as from the plasma membrane of mammalian cells (1,2). There is also evidence that intra-MVB sorting is a primary significant mechanism for terminating receptor-mediated signaling by the EGF receptoir tyrosine kinases in the endocytic pathway (2,42). Thus we speculate anticipate that the ESCRT / MVB system, besides its established function in driving ubiquitin-directed destruction of various integral membrane proteins, that serves additional role(s) in controlling the duration or subcellular localization of specific receptor-mediated signaling activities. the sequential organization of biochemically discrete molecular sorting operations, established in the present study, likely provides animal cells with an additional level of specificity in regulating particular members of the largest known family of signaling receptors.

Materials and Methods

Cell culture, cDNA constructs and transfection

The Myc tagged inactive mutant AIP4 has been previously described (30) and was a gift from Adriano Marchese (Loyola University, Chicago IL). GFP-tagged Rab5 cDNA was a gift from Marino Zerial (Max Planck Institute of Molecular Cell Biology and Genetics, Germany), and the Q79L mutation was made by site-directed mutagenesis (Stratagene), HRS cDNA was a gift from Harold Stenmark (Norwegian Radium Hospital), Nedd-4-1-C/A mutant was a gift from Laurant Coscoy (University of California, Berkeley), and the mCherry cDNA was a gift from Roger Tsien (University of California, San Diego). PCR was used to remove the stop codon from mCherry, and the resulting fragment was cloned into pcDNA3.0 (Invitrogen). This vector was then used to construct N-terminal fusions of HRS, Nedd4-1-C/A and AIP4-C/A. N-terminal FLAG-tagged, and C-terminal HA-tagged versions of wild type and lysine-mutant δ-opioid receptor have been previously described as F-DOR-HA and F-DOR-0cK-HA (24). C-terminal GFP-tagged fusion constructs were generated from these constructs by PCR, introducing an AgeI restriction site into the reverse primer at the appropriate location, and ligating in-frame into pEGFP-N1 (Clontech). We constructed pHluorin-tagged receptors using PCR to replace the EGFP coding sequence with superecliptic pHluorin (41,46). All cDNA constructs were verified by sequencing (ElimBio, CA). Human embryonal kidney 293 (HEK293) cells (ATCC) were maintained in Dulbecco's modified Eagles medium supplemented with 10% fetal bovine serum (University of California, San Francisco, Cell Culture Facility). For transient expression, cells were transfected using Lipofectamine 2000 (Invitrogen) according to manufacturers' instructions. Cells expressing FLAG-tagged receptors were harvested by washing with EDTA and plated in 60-mm dishes at 80% confluency, before transfection with plasmid DNA. Cells were reseeded into poly-lysine coated 6-well or 24 well plates and cultured for a further 24 hours before experiments. For stable expression, clonal selection was carried out using 500 μg/ml G418 (Geneticin, Gibco), and clones were selected for study based on comparable levels of receptor expression as determined by saturation binding analysis using ^{3}H-diprenorphine as described previously (24). Expression levels used in this study were between 0.5 and 2 pmol / mg; this is within the range of endogenous opioid receptor expression in brain tissue (20), and does not saturate the endocytic machinery in HEK293 cells (23,24).

Biochemical detection of receptor proteolysis and protein levels by immunoblotting

Immunoblotting to assess total cellular receptor levels was carried out as previously described (24). Briefly, cell monolayers were washed three times in ice-cold phosphate buffered saline (PBS) and lysed in extraction buffer (0.5% Triton X-100, 150 mM NaCl, 25 mM KCl, 25 mM Tris pH 7.4, 1 mM EDTA) supplemented with a standard protease inhibitor cocktail (Roche). Extracts were clarified by centrifugation (12,000 x g for 10 minutes), and then mixed with SDS sample buffer for denaturation. Proteins present in the extracts were resolved by SDS-PAGE using 4-12% Bis-Tris gels (Nu-PAGE, Invitrogen), transferred to nitrocellulose membranes, and probed for protein by immunoblotting using horseradish peroxidase-conjugated sheep anti-mouse IgG or donkey anti-rabbit IgG (Amersham Biosciences), and SuperSignal detection reagent (Pierce). Apparent molecular mass was estimated using commercial protein standards (SeeBlue Plus2, Invitrogen). Band intensities of unsaturated immunoblots were analyzed and quantified by densitometry using FluorChem 2.0 software (AlphaInnotech Corp.). Antibodies used were anti-FLAG-M1 (Sigma) and anti-HA-11 (Covance).

Biochemical detection of receptor proteolytic fragments by immunoblotting

Following lysis as above, samples were immunoprecipitated with anti-HA-11 and protein A/G agarose beads. Washed beads were deglycosylated by the addition of 500 units of PNGase

F (NEB) and incubated for 1 hour at 37 C before the elution with SDS sample buffer, resolving by SDS-PAGE and then transferred to nitrocellulose membranes, and probed for HA-tagged receptor (anti-HA-HRP antibody, clone 3F10, Roche).

Spinning-disc confocal microscopy of living cells

For live imaging, HEK 293 transiently-transfected with the indicated N-terminally FLAG-tagged, C-terminally GFP-tagged receptor constructs were plated onto polylysine-coated glass coverslips (Corning Glass). Cells were incubated in the presence of 10 μM DADLE for 90 min prior to imaging. Cells were imaged in Dulbecco's Modified Eagle Medium without Phenol Red (UCSF Cell Culture Facility) supplemented with 1% fetal bovine serum (UCSF Cell Culture Facility) and 30mM Hepes adjusted to pH 7.4. Live cell imaging was performed using a Yokogawa CSU22 Spinning Disk Confocal (Solamere Technology Group) on a Nikon TE2000U inverted microscope. Cells were visualized using a 100 X 1.49 NA TIRF objective and illuminated with a 488nm Ar Laser (Melles Griot). Time-lapse sequences were acquired at a continuous rate of 5 frames per second and acquired images were analyzed with Image J software (Wayne Rasband, National Institutes of Health, Bethesda, MD). Quantification was conducted on raw data representing confocal cross-sections of individual endosomes. For each endosome, straight-line selections were drawn across the diameter and pixel intensities across the line were measured. Endosomal diameter was normalized to account for endosomes varying in size. The pixel numbers with the first and second maximum pixel intensities, corresponding to pixels on the limiting membrane of the endosome, were normalized to 0 and 100, respectively. The location across the line of pixel 0 was then subtracted from each pixel situated on the line and this value was divided by the total diameter (in pixels) of the endosome. This generated normalized pixel distances corresponding to distance across the line occupied by each pixel, expressed as a percentage. Average background fluorescence was subtracted from raw pixel intensity values. The pixel intensities for the pixel numbers normalized to 0 and 100 were also normalized to 0 and 100, respectively, generating normalized fluorescence values. The background-corrected pixel intensity values corresponding to pixels that lay 40–60% across the endosomal diameter were averaged, generating a middle fluorescence value for each endosome. Middle fluorescence values were compiled across multiple cells and the mean values quantified for each condition are shown. Representative live images shown were rendered using Adobe Photoshop software.

Live Cell Imaging using the pH-sensitive GFP variant

HEK 293 cells transiently-transfected with the indicated N-terminally FLAG-tagged, C-terminally ecliptic GFP variant-tagged receptor constructs were plated onto polylysine-coated glass coverslips (Corning Glass). Cells were incubated in the presence of 10 μM DADLE for 90 min prior to imaging. Cells were imaged for 10s and then 1mM chloroquine was added to cells while image acquisition continued. Quantification was conducted on raw data representing confocal cross-sections of individual endosomes. For each endosome, selections were drawn around each individual endosome and the mean fluorescence values were background corrected. To measure the chloroquine-induced increase in fluorescence inside the endosomal lumen, the minimum average fluorescence value in the first half of the image sequence was identified and fluorescence values for the three frames before and after this frame were averaged. This mean was the average minimum fluorescence. The maximum average fluorescence value in the second half of the image sequence was determined and fluorescence values for the three frames before and after this frame were averaged. This mean was the average maximum fluorescence. To calculate the fold increase for each individual endosome, the average maximum fluorescence value was divided by the average minimum fluorescence value. Fold increase in fluorescence measurements were compiled across multiple cells and the mean values quantified for each condition are shown.

Laser-scanning confocal microscopy of fixed specimens

HEK293 cells were transiently transfected with either F-DOR-HA or F-DOR-0cK-HA and then plated on polylysine-coated glass coverslips (Corning). Cells were 'fed' with Rabbit anti-FLAG antibody (1μg/ml, Sigma) for 30 minutes to label the surface pool of receptors, before being left untreated, incubated in the presence of 10 μM DADLE for 30 minutes, or incubated with agonist followed by incubation with antagonist (10μM Naloxone) for 60 minutes, before fixation with 4% formaldehyde and permeablization with 0.1% Triton-X100 in PBS. Cells were labeled using mouse anti-HA-11 (Covance), followed by secondary detection using Alexa488-conjugated anti-mouse and Alexa555 anti-rabbit secondary antibodies (Invitrogen). Specimens were imaged by confocal fluorescence microscopy using a Zeiss LSM 510 microscope fitted with a Zeiss 63 x NA1.4 objective operated in single photon mode, with standard filter sets verified for lack of detectable cross-channel bleed through and standard (1 Airy disc) pinhole. Acquired optical sections were analyzed with LSM Image Examiner (Zeiss) and rendered with Adobe Photoshop software.

Quantification of receptor recycling by fluorescence flow cytometry

A previously described flow cytometric method for accurately measuring opioid receptor recycling (18) was used with minor variation (32). Briefly, surface N-terminally FLAG-tagged and C-terminally HA-tagged DOR and DOR0cK receptors stably expressed in HEK 293 cells were labeled with M1 anti–FLAG antibody (1 mg/mL, Sigma) conjugated to Alexa647 isothiocyanate (Invitrogen/ Molecular Probes) according to manufacturer's instructions. Cells were incubated with 10 μM DADLE for 30 min at 37 °C to drive receptor internalization to steady state, and cells were rinsed three times with calcium and magnesium-free PBS supplemented with 0.4% EDTA to dissociate antibody from receptors remaining at the plasma membrane and therefore specifically label internalized receptors. To determine whether the presence of intracellular lysine residues affects recycling of receptors, cells were incubated at 37 °C in EDTA-supplemented PBS with 10μM naloxone (to prevent residual agonist effects) for the indicated time periods. Monolayers were chilled to 4 °C, lifted, and analyzed by flow cytometry to detect antibody bound to internalized receptors remaining within the cell. Transferrin receptor recycling was measured over the same time scale using a previously described 'pulse-chase' method (47) based on efflux of labeled transferrin bound to the internalized receptor pool, and adapted to flow cytometry using Alexa488-conjugated diferric transferrin (Invitrogen, 1 μg/mL) as described previously (32).

Cryosectioning and immunoelectron microscopy

Cells were fixed with 4% paraformaldehyde in 0.1 M phosphate buffer pH 7.4, infused with 2.3 M sucrose and supported in 12% gelatin. Sections (70 nm) were cut at −120°C and picked up in 1:1 sucrose:methylcellulose. For labeling, primary antibody was followed by rabbit anti-mouse intermediate antibody (DAKO) and sections were then labeled using protein A gold as described (48). Images were obtained using a Tecnai T12 transmission electron microscope (FEI, Netherlands) and captured using a Morada CCD camera (Olympus-SIS).

Statistical analysis

Quantitative data were averaged across multiple independent experiments, with the number of experiments specified in the corresponding figure legend. Unless indicated otherwise, error bars represent the standard error of the mean determined after compiling mean determinations across experiments. The statistical significance of the indicated differences were was analyzed using the appropriate variations of two-way ANOVA and post-test, or Student's t test, as specified in the figure legends and calculated using Prism 4.0 software (GraphPad Software, Inc). The relative significance of each of the reported differences is

specified by calculated p values that are also listed in the figure legends, and annotated graphically in the figures.

Supplementary Material

Refer to Web version on PubMed Central for supplementary material.

Acknowledgments

This work was supported by grants from the NIH (DA010711 and DA012864 to MvZ) and the UK Medical Research Council to MM and IW. AGH is a recipient of a predoctoral fellowship from the US National Science Foundation. The authors gratefully acknowledge Kurt Thorn and the Nikon Imaging Center at UCSF for useful advice, and for providing access to fluorescence imaging instrumentation. We thank Adriano Marchese and Harald Stenmark for valuable discussion and sharing important essential reagents, Scott Emr, Manoj Pathenveedu, Michael Tanowitz and Paul Temkin for critical comments and suggestions, and Aaron Marley, Laurant Coscoy, Roger Tsien and Marino Zerial for generously providing constructs used in this study.

Abbreviations

ESCRT	endosomal sorting complex required for transport
GPCR	G protein-coupled receptor
ILV	intralumenal vesicle
MVB	multivesicular body

References

1. Sorkin A, von Zastrow M. Endocytosis and signalling: intertwining molecular networks. Nat Rev Mol Cell Biol. 2009; 10(9):609–622. [PubMed: 19696798]
2. Miaczynska M, Pelkmans L, Zerial M. Not just a sink: endosomes in control of signal transduction. Curr Opin Cell Biol. 2004; 16(4):400–406. [PubMed: 15261672]
3. Ferguson SS, Zhang J, Barak LS, Caron MG. Molecular mechanisms of G protein-coupled receptor desensitization and resensitization. Life Sci. 1998; 62(17–18):1561–1565. [PubMed: 9585136]
4. Carman CV, Benovic JL. G-protein-coupled receptors: turn-ons and turn-offs. Current Opinion in Neurobiology. 1998; 8(3):335–344. [PubMed: 9687355]
5. Hanyaloglu AC, von Zastrow M. Regulation of GPCRs by endocytic membrane trafficking and its potential implications. Annu Rev Pharmacol Toxicol. 2008; 48:537–568. [PubMed: 18184106]
6. Marchese A, Paing MM, Temple BR, Trejo J. G protein-coupled receptor sorting to endosomes and lysosomes. Annu Rev Pharmacol Toxicol. 2008; 48:601–629. [PubMed: 17995450]
7. Hicke L. A new ticket for entry into budding vesicles-ubiquitin. Cell. 2001; 106(5):527–530. [PubMed: 11551499]
8. Shenoy SK. Seven-transmembrane receptors and ubiquitination. Circ Res. 2007; 100(8):1142–1154. [PubMed: 17463329]
9. Kirkin V, Dikic I. Role of ubiquitin- and Ubl-binding proteins in cell signaling. Curr Opin Cell Biol. 2007; 19(2):199–205. [PubMed: 17303403]
10. Hislop JN, Von Zastrow M. Role of Ubiquitination in Endocytic Trafficking of G-Protein-Coupled Receptors. Traffic. 2010
11. Katzmann DJ, Babst M, Emr SD. Ubiquitin-dependent sorting into the multivesicular body pathway requires the function of a conserved endosomal protein sorting complex, ESCRT-I. Cell. 2001; 106(2):145–155. [PubMed: 11511343]
12. Hurley JH, Wendland B. Endocytosis: driving membranes around the bend. Cell. 2002; 111(2): 143–146. [PubMed: 12408856]
13. Hicke L, Dunn R. Regulation of membrane protein transport by ubiquitin and ubiquitin-binding proteins. Annu Rev Cell Dev Biol. 2003; 19:141–172. [PubMed: 14570567]

14. Huang F, Kirkpatrick D, Jiang X, Gygi S, Sorkin A. Differential regulation of EGF receptor internalization and degradation by multiubiquitination within the kinase domain. Mol Cell. 2006; 21(6):737–748. [PubMed: 16543144]
15. Saksena S, Sun J, Chu T, Emr SD. ESCRTing proteins in the endocytic pathway. Trends Biochem Sci. 2007; 32(12):561–573. [PubMed: 17988873]
16. Marchese A, Benovic JL. Agonist-promoted ubiquitination of the G protein-coupled receptor CXCR4 mediates lysosomal sorting. J Biol Chem. 2001; 276(49):45509–45512. [PubMed: 11641392]
17. Jacob C, Cottrell GS, Gehringer D, Schmidlin F, Grady EF, Bunnett NW. c-Cbl mediates ubiquitination, degradation, and down-regulation of human protease-activated receptor 2. J Biol Chem. 2005; 280(16):16076–16087. [PubMed: 15708858]
18. Tsao PI, von Zastrow M. Type-specific sorting of G protein-coupled receptors after endocytosis. J Biol Chem. 2000; 275(15):11130–11140. [PubMed: 10753919]
19. Law PY, Wong YH, Loh HH. Molecular mechanisms and regulation of opioid receptor signaling. Annu Rev Pharmacol Toxicol. 2000; 40:389–430. [PubMed: 10836142]
20. Scherrer G, Tryoen-Toth P, Filliol D, Matifas A, Laustriat D, Cao YQ, Basbaum AI, Dierich A, Vonesh JL, Gaveriaux-Ruff C, Kieffer BL. Knockin mice expressing fluorescent delta-opioid receptors uncover G protein-coupled receptor dynamics in vivo. Proc Natl Acad Sci U S A. 2006; 103(25):9691–9696. [PubMed: 16766653]
21. Pradhan AA, Becker JA, Scherrer G, Tryoen-Toth P, Filliol D, Matifas A, Massotte D, Gaveriaux-Ruff C, Kieffer BL. In vivo delta opioid receptor internalization controls behavioral effects of agonists. PLoS One. 2009; 4(5):e5425. [PubMed: 19412545]
22. Tanowitz M, Von Zastrow M. Ubiquitination-independent trafficking of G protein-coupled receptors to lysosomes. J Biol Chem. 2002; 277(52):50219–50222. [PubMed: 12401797]
23. Hislop JN, Marley A, Von Zastrow M. Role of mammalian vacuolar protein-sorting proteins in endocytic trafficking of a non-ubiquitinated G protein-coupled receptor to lysosomes. J Biol Chem. 2004; 279(21):22522–22531. [PubMed: 15024011]
24. Hislop JN, Henry AG, Marchese A, von Zastrow M. Ubiquitination regulates proteolytic processing of G protein-coupled receptors after their sorting to lysosomes. J Biol Chem. 2009; 284(29):19361–19370. [PubMed: 19433584]
25. Whistler JL, Enquist J, Marley A, Fong J, Gladher F, Tsuruda P, Murray SR, Von Zastrow M. Modulation of postendocytic sorting of G protein-coupled receptors. Science. 2002; 297(5581): 615–620. [PubMed: 12142540]
26. Simonin F, Karcher P, Boeuf JJ, Matifas A, Kieffer BL. Identification of a novel family of G protein-coupled receptor associated sorting proteins. J Neurochem. 2004; 89(3):766–775. [PubMed: 15086532]
27. Marley A, von Zastrow M. Dysbindin promotes the post-endocytic sorting of G protein-coupled receptors to lysosomes. PLoS One. 2010; 5(2):e9325. [PubMed: 20174469]
28. Petaja-Repo UE, Hogue M, Laperriere A, Bhalla S, Walker P, Bouvier M. Newly synthesized human delta opioid receptors retained in the endoplasmic reticulum are retrotranslocated to the cytosol, deglycosylated, ubiquitinated, and degraded by the proteasome. J Biol Chem. 2001; 276(6):4416–4423. [PubMed: 11054417]
29. Chaturvedi K, Bandari P, Chinen N, Howells RD. Proteasome involvement in agonist-induced down-regulation of mu and delta opioid receptors. J Biol Chem. 2001; 276(15):12345–12355. [PubMed: 11152677]
30. Marchese A, Raiborg C, Santini F, Keen JH, Stenmark H, Benovic JL. The E3 ubiquitin ligase AIP4 mediates ubiquitination and sorting of the G protein-coupled receptor CXCR4. Dev Cell. 2003; 5(5):709–722. [PubMed: 14602072]
31. Chen L, Davis NG. Ubiquitin-independent entry into the yeast recycling pathway. Traffic. 2002; 3(2):110–123. [PubMed: 11929601]
32. Yudowski GA, Puthenveedu MA, Henry AG, von Zastrow M. Cargo-mediated regulation of a rapid Rab4-dependent recycling pathway. Mol Biol Cell. 2009; 20(11):2774–2784. [PubMed: 19369423]

33. Maxfield FR, McGraw TE. Endocytic recycling. Nat Rev Mol Cell Biol. 2004; 5(2):121–132. [PubMed: 15040445]
34. Krisch B, Feindt J, Mentlein R. Immunoelectronmicroscopic analysis of the ligand-induced internalization of the somatostatin receptor subtype 2 in cultured human glioma cells. J Histochem Cytochem. 1998; 46(11):1233–1242. [PubMed: 9774622]
35. Volpicelli LA, Lah JJ, Levey AI. Rab5-dependent trafficking of the m4 muscarinic acetylcholine receptor to the plasma membrane, early endosomes, and multivesicular bodies. J Biol Chem. 2001; 276(50):47590–47598. [PubMed: 11590149]
36. Fraile-Ramos A, Pelchen-Matthews A, Kledal TN, Browne H, Schwartz TW, Marsh M. Localization of HCMV UL33 and US27 in endocytic compartments and viral membranes. Traffic. 2002; 3(3):218–232. [PubMed: 11886592]
37. Slagsvold T, Marchese A, Brech A, Stenmark H. CISK attenuates degradation of the chemokine receptor CXCR4 via the ubiquitin ligase AIP4. Embo J. 2006; 25(16):3738–3749. [PubMed: 16888620]
38. Wegener CS, Malerod L, Pedersen NM, Prodiga C, Bakke O, Stenmark H, Brech A. Ultrastructural characterization of giant endosomes induced by GTPase-deficient Rab5. Histochem Cell Biol. 2009
39. Trajkovic K, Hsu C, Chiantia S, Rajendran L, Wenzel D, Wieland F, Schwille P, Brugger B, Simons M. Ceramide triggers budding of exosome vesicles into multivesicular endosomes. Science. 2008; 319(5867):1244–1247. [PubMed: 18309083]
40. van der Goot FG, Gruenberg J. Intra-endosomal membrane traffic. Trends Cell Biol. 2006; 16(10): 514–521. [PubMed: 16949287]
41. Miesenbock G, De Angelis DA, Rothman JE. Visualizing secretion and synaptic transmission with pH-sensitive green fluorescent proteins. Nature. 1998; 394(6689):192–195. [PubMed: 9671304]
42. Futter CE, Collinson LM, Backer JM, Hopkins CR. Human VPS34 is required for internal vesicle formation within multivesicular endosomes. J Cell Biol. 2001; 155(7):1251–1264. [PubMed: 11756475]
43. Raiborg C, Stenmark H. The ESCRT machinery in endosomal sorting of ubiquitylated membrane proteins. Nature. 2009; 458(7237):445–452. [PubMed: 19325624]
44. Cottrell GS, Padilla B, Pikios S, Roosterman D, Steinhoff M, Gehringer D, Grady EF, Bunnett NW. Ubiquitin-dependent down-regulation of the neurokinin-1 receptor. J Biol Chem. 2006; 281(38):27773–27783. [PubMed: 16849335]
45. Rios CD, Jordan BA, Gomes I, Devi LA. G-protein-coupled receptor dimerization: modulation of receptor function. Pharmacol Ther. 2001; 92(2–3):71–87. [PubMed: 11916530]
46. Sankaranarayanan S, De Angelis D, Rothman JE, Ryan TA. The use of pHluorins for optical measurements of presynaptic activity. Biophys J. 2000; 79(4):2199–2208. [PubMed: 11023924]
47. Dunn KW, McGraw TE, Maxfield FR. Iterative fractionation of recycling receptors from lysosomally destined ligands in an early sorting endosome. Journal of Cell Biology. 1989; 109(6 Pt 2):3303–3314. [PubMed: 2600137]
48. Slot JW, Geuze HJ, Gigengack S, Lienhard GE, James DE. Immuno-localization of the insulin regulatable glucose transporter in brown adipose tissue of the rat. J Cell Biol. 1991; 113(1):123–135. [PubMed: 2007617]

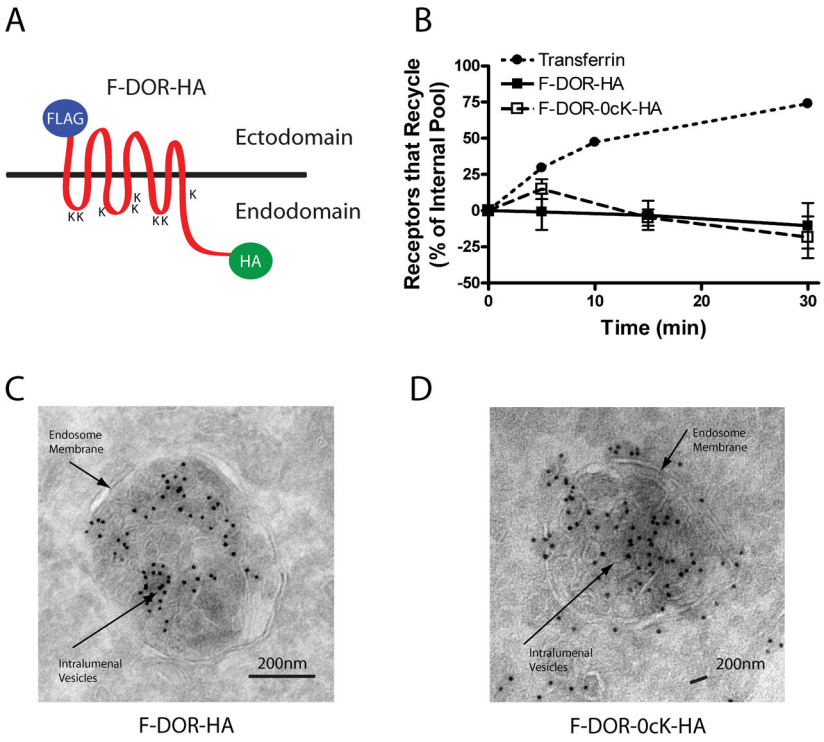

Figure 1. Both DOR and DOR-0cK are efficiently excluded from the recycling pathway and can undergo transfer in ILVs of endosomes

A) Schematic representation of the N and C terminally tagged DOR, indicating the positions of the respective tags and lysine residues (K) **B)** Recycling time course of FLAG-DOR-HA and FLAG-DOR-0cK-HA receptors relative to transferrin receptors. For the opioid receptors, internalization of antibody-labeled receptors was carried out by 30-min pre-incubation with 10μM DADLE. Cells were washed, incubated in the presence of 10μM naloxone, and antibody efflux was assayed at the indicated time points. Recycling of transferrin receptors was estimated by efflux of Alexa488-conjugated transferrin. Points represent mean determinations calculated from three independent experiments. Error bars represent the SEM calculated across experiments (n = 3). HEK293 cells stably expressing F-DOR-HA (**A**) or F-DOR-0cK-HA (**C and D**) were treated with 10μM DADLE for 90 minutes before fixation and preparation for cryosectioning, immunolabeling and electron microscopy as described in *Materials and Methods*. Shown are representative micrographs using anti-HA labeled with 10nm gold particles. Both F-DOR-HA and F-DOR-0cK-HA were resolved in association with intralumenal vesicle membranes of multivesicular bodies. Scale bars indicate 200 nm.

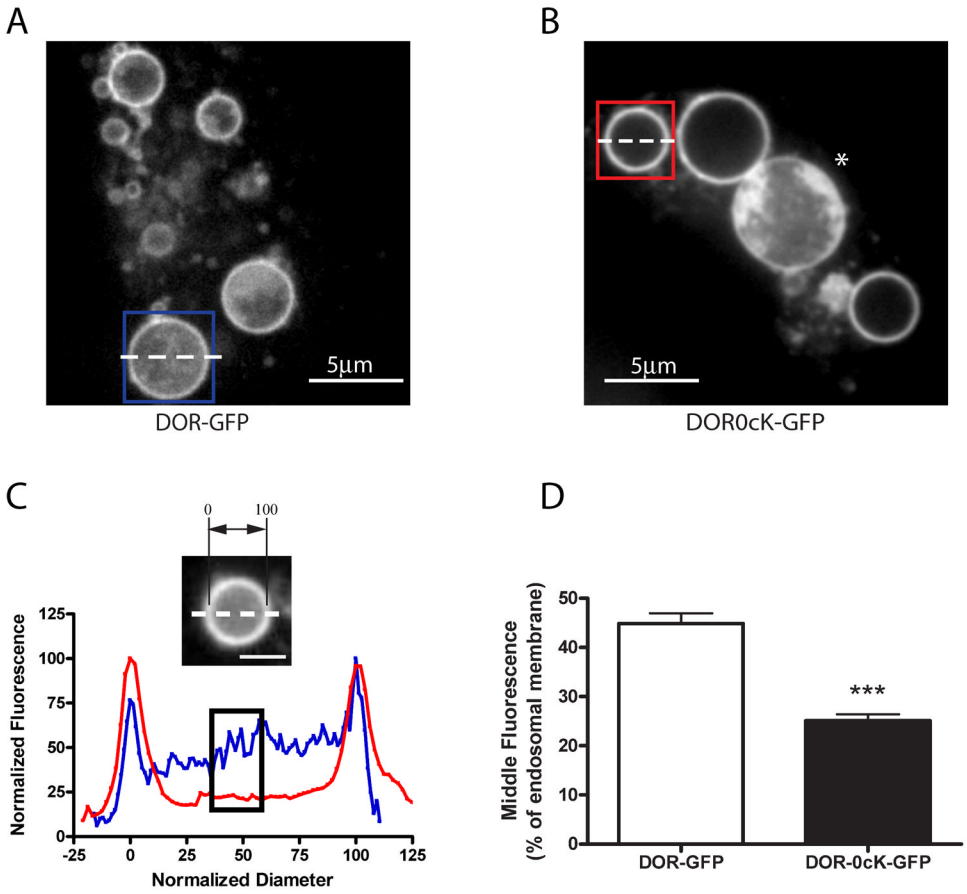

Figure 2. Enlargement of endosomes by Rab5 manipulation illustrates lysyl-mutant DORs differ in their extent of transfer to ILVs

A and B) HEK293 cells were transiently transfected with CFP-Rab5Q79L and either F-DOR-GFP (**A**) or F-DOR-0cK-GFP (**B**), and replated onto to coverslips before treatment for 90 minutes with 10µM DADLE. Cells were then imaged by spinning disc confocal microscopy as described in *Materials and Methods*. Shown are representative still images of the representative acquired image series, scale bars indicate 5µm. **C)** Line scan analysis to quantify receptor localization to the intralumenal compartment. Normalized diameter represents the diameter of the endosome shown, where 0 and 100 correspond to the pixel distances with the first and second maximum pixel intensities measured across the dashed line, respectively (see inset image). Blue and red traces represent the normalized pixel intensity measured across the dashed line in the blue and red boxes in A and B respectively, where the maximum pixel intensity across the line is normalized to 100. The black box highlights the normalized fluorescence values of pixels from 40 to 60% of the normalized diameter. **D)** Compiled results of line scan analysis (mean and SEM, *** $p<0.001$, Student's t-test, n= 88 endosomes, ≥12 cells).

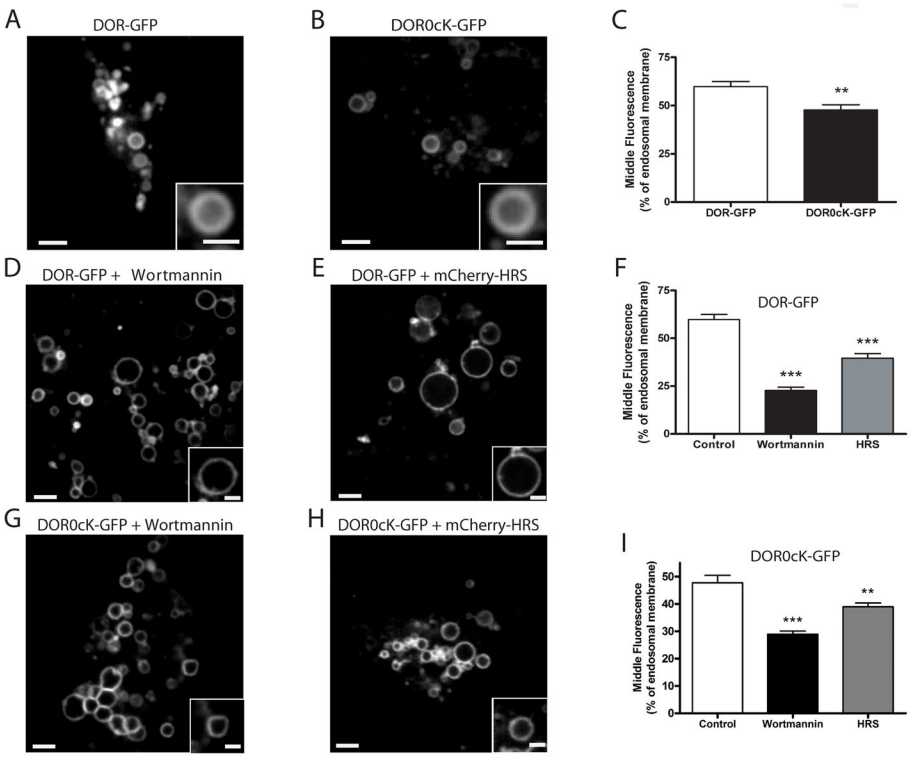

Figure 3. Differences in the extent of DOR transfer to ILVs can be detected by live-cell imaging of non-enlarged endosomes

A and B) Live cell imaging of non-enlarged endosomes in HEK293 cells expressing either F-DOR-GFP (**A**) or F-DOR-0cK-GFP (**B**) imaged live by spinning disc confocal microscopy after exposure for 90 minutes to 10μM DADLE. Shown are representative still images of the representative acquired image series (see Supplemental Movie 1 and 2. Scale bars are 2μm and 1μm for the insets. **C)** Quantification of the middle fluorescence, or percentage of endosomal membrane, measured from individual endosomes. Mean and SEM of middle fluorescence values are shown for F-DOR-GFP transfected cells (DOR-GFP, n= 12 cells, 50 endosomes) and F-DOR0cK-GFP transfected cells (** $p<0.01$, Student's t-test, n=59 endosomes, 13 cells). **D-F)** The same experiment in cells transfected with F-DOR-GFP and pretreated with 500nM wortmannin (**D)** or transfected 48 hours before DADLE addition with mCherry-HRS (**E)**. Scale bar on overall image = 2μm and on inset = 1 μm. **F)** Fluorescence intensity was measured through the center of the endosome as in (A-C) and the mean internal fluorescence is expressed as a percentage of that of the membrane of wortmannin pre-treated F-DOR-GFP transfected cells (Wortmannin, unpaired t-test; ***, $p<0.0001$, n= 11 cells, 50 endosomes), and F-DOR-GFP and mCherry-HRS transfected cells (HRS, unpaired t-test; ***, $p<0.0001$, n= 10 cells, 64 endosomes). **D)** The same experiment in cells transfected with F-DOR0cK-GFP and pretreated with 500nM wortmannin **(G)** or transfected 48 hours before DADLE addition with mCherry-HRS **(H)**. Scale bar on overall image = 2μm and on inset = 1 μm. **I)** Quantification of the middle fluorescence. Mean and SEM of middle fluorescence values are shown for wortmannin pre-treated F-DOR0cK-GFP transfected cells (Wortmannin, unpaired t-test; ***, $p<0.001$, n= 11 cells, 92 endosomes), and F-DOR0cK-GFP and mCherry-HRS transfected cells (HRS, unpaired t-test; **, $p<0.01$, n= 10 cells, 116 endosomes).

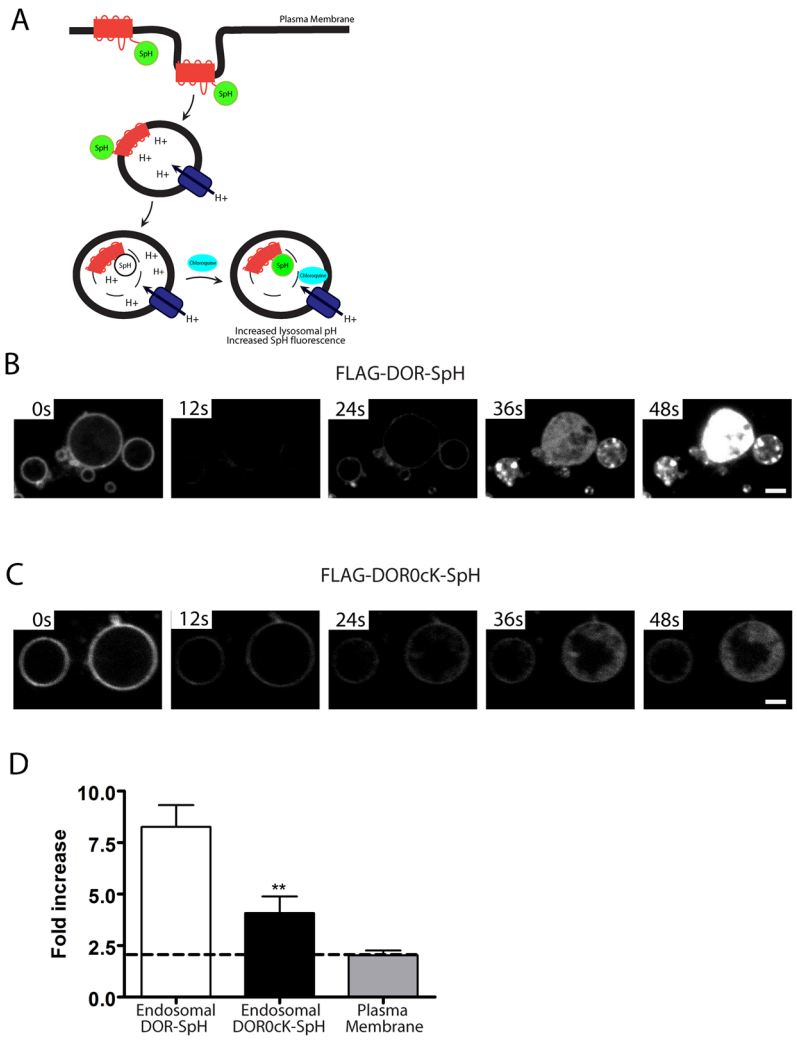

Figure 4. Intralumenal wild -type and lysyl-mutant receptors visualized using a pH-sensitive GFP variant

A) Schematic of experimental setup following receptors fused to the GFP variant (ecliptic pHluorin) which fluoresce when located in the cytoplasm but whose fluorescence is efficiently quenched when exposed to the acidic environment of the endosome lumen. Addition of the weak base chloroquine neutralizes endosomal pH and reveals any tagged receptors present in the endosome lumen. **B and C)** HEK293 cells were transiently transfected with CFP-Rab5Q79L and either F-DOR-SpH (**B**) or F-DOR-0cK-SpH **(C)**, and replated onto to coverslips before treatment for 90 minutes with 10μM DADLE. Cells were then imaged at a rate of 5 frames per second by spinning disc confocal microscopy and treated with 1mM chloroquine after 50 frames. Image sequences are shown for cells expressing F-DOR-SpH (**B**) or F-DOR-0cK-SpH **(C),** see Supplemental Movies 3 and 4 for full sequence**. D)** Quantification of the chloroquine-induced increase in fluorescence intensity. Mean and SEM are shown for F-DOR-SpH (Endosomal DOR-SpH, n= 8 cells, 24 endosomes) and F-DOR0cK-SpH containing endosomes (Endosomal DOR0cK-SpH, unpaired t-test; ***, p<0.01, n= 7 cells, 22 endosomes), and F-DOR-SpH expressed on the plasma membrane (Plasma Membrane, n= 11 cells). Scale bar = 2 μm.

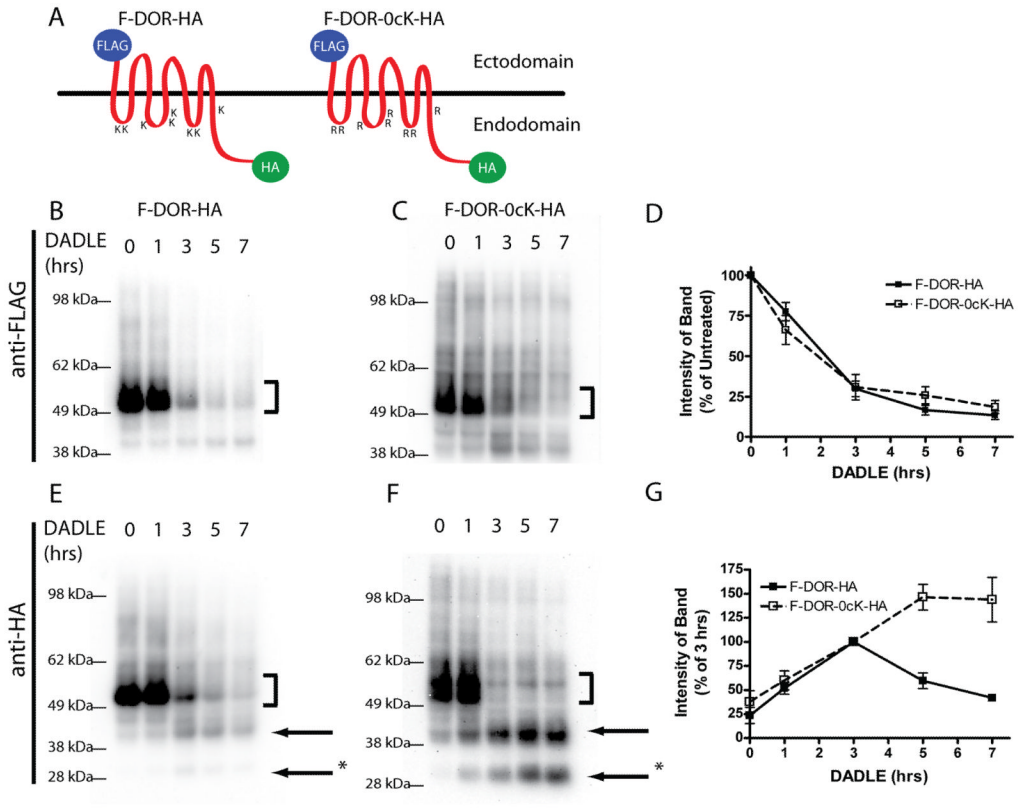

Figure 5. Differential proteolysis of N and C-terminal fragments of DOR and DOR-0cK

A) Schematic representation of doubly-tagged receptor constructs of F-DOR-HA and F-DOR-0cK-HA indicating the N-terminal and C-terminal locations of the FLAG and HA epitope tags, respectively. HEK293 cells stably expressing F-DOR-HA (**C and F**) or F-DOR-0cK-HA (**D and G**) were incubated with 10μM DADLE for the indicated time period before lysis and division into two identical samples. Shown are representative anti-FLAG blots (**C and D**) and anti-HA blots (**F and G**) as indicated. Bracket indicates position of the full-length receptor species. Arrows denote major proteolytic cleavage products. **E)** Blots generated in multiple experiments were scanned to estimate the amount of FLAG-tagged receptor remaining at each time point after incubation in the presence of 10μM DADLE, expressed as a percentage of that in cells not exposed to agonist, results were pooled and averaged across multiple experiments (shown are mean and SEM, n=5). **H)** Anti-HA blots were scanned and the relative immunoreactivity of one proteolytic product (denoted *) was measured and expressed as a percentage of density at 3 hrs, where the band for DOR was most intense. Closed symbols indicate the degradation curve measured for F-DOR-HA, open symbols indicate the degradation curve measured in cells transfected with F-DOR-0cK-HA (mean and SEM, n=5)

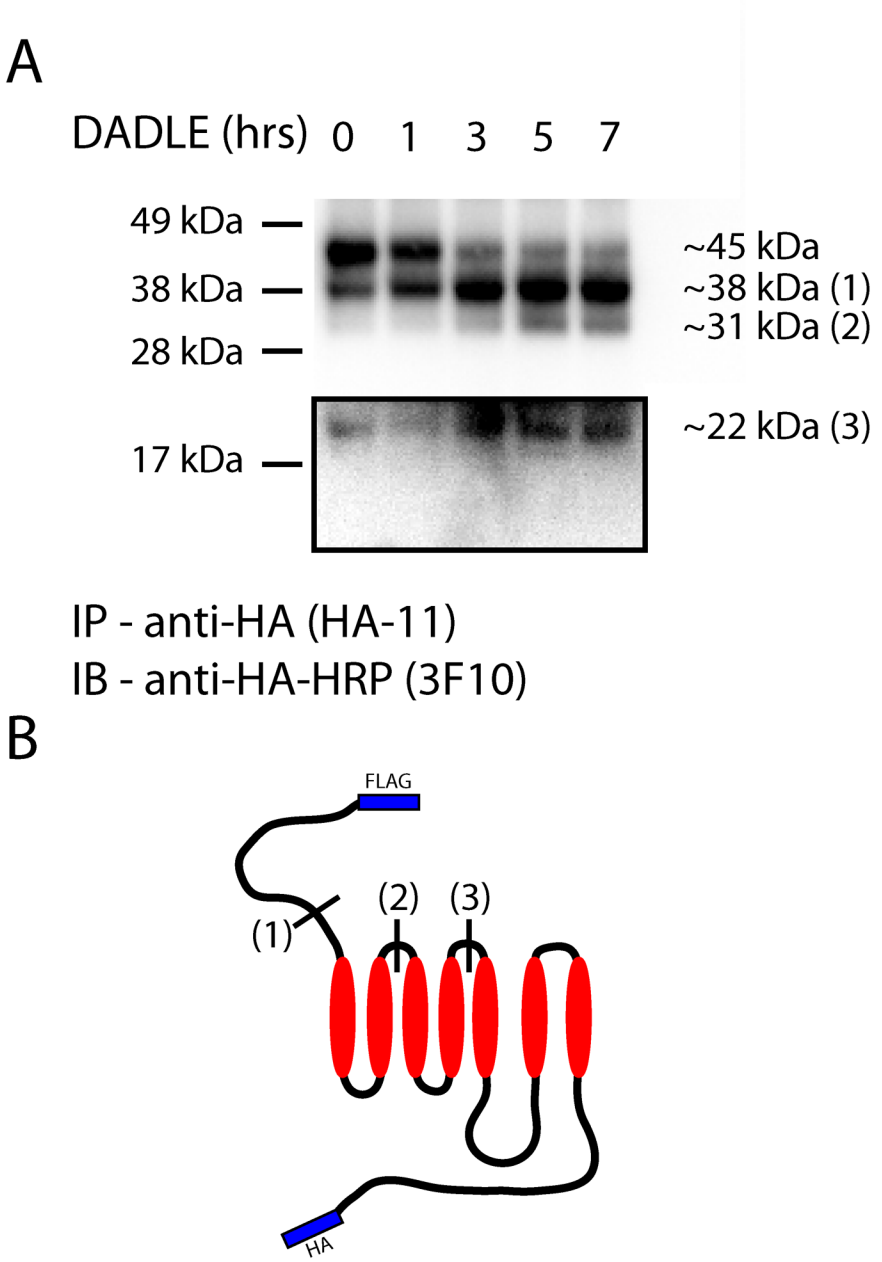

Figure 6. Analysis of the proteolytic fragmentation of lysine-mutant DORs show delayed destruction specifically of the receptor endodomain

HEK293 cells stably expressing F-DOR-0cK-HA were incubated with 10μM DADLE for the indicated time period before lysis. HA-linked fragments were immunoprecipitated, treated with PNGaseF, and separated via SDS-PAGE. Shown is a representative anti-HA blot (**A).** Proteolytic fragments resolved to the indicated sizes, corresponding topologically as diagrammed in **(B).**

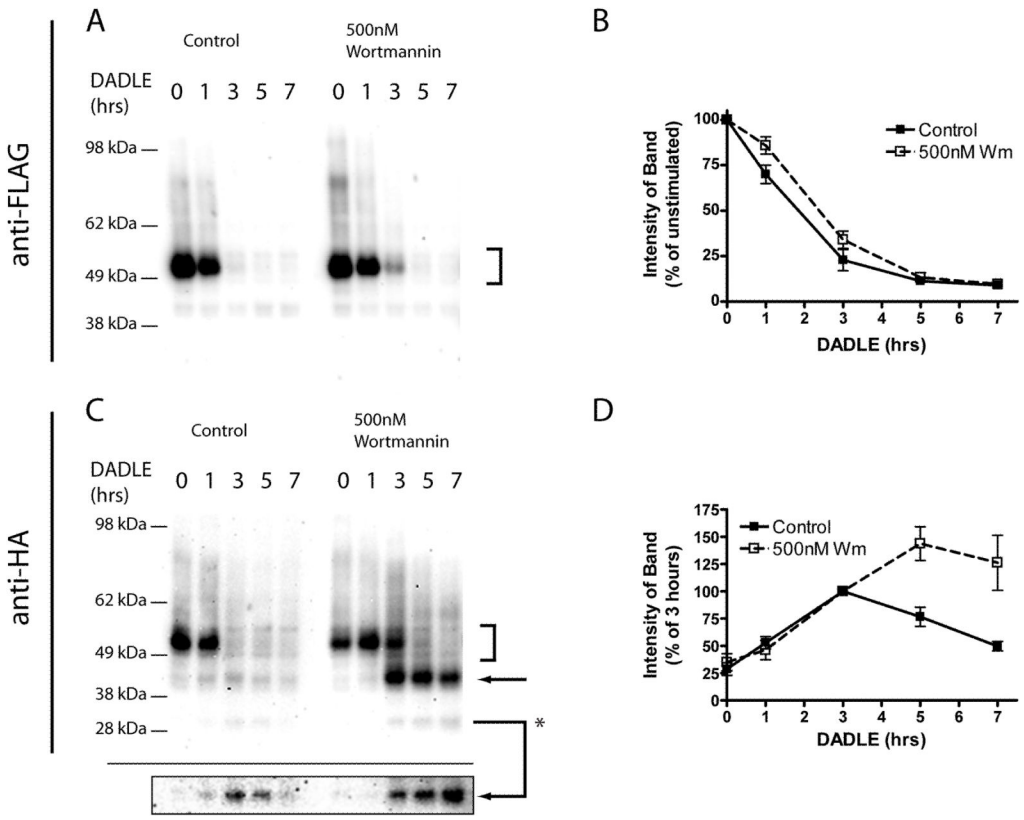

Figure 7. Persistence of proteolytic cleavage products is mimicked by treatment with Wortmannin

HEK293 cells stably expressing F-DOR-HA were pretreated with vehicle control (DMSO) or 500nM Wortmannin before incubation with 10μM DADLE for the indicated time period before lysis and division into two identical samples. Shown are representative anti-FLAG (**A**) or anti-HA (**C**) Western blots. Arrows denote major proteolytic cleavage products, and the highlighted box shows a darker exposure of the proteolytic product at ~30kDa. Blots generated across multiple experiments were scanned and densitometry performed to estimate the amount of FLAG-tagged receptors remaining at each time point relative to agonist naïve cells (**C**), and the relative abundance of one anti-HA immunoreactive proteolytic product (denoted *) expressed as a percentage of density at 3 hrs agonist treatment (**D**). Shown are the mean and SEM of multiple experiments (n=6); closed symbols indicate densitometry in control, DMSO treated cells, and open symbols indicate cells treated with 500nM Wortmannin.

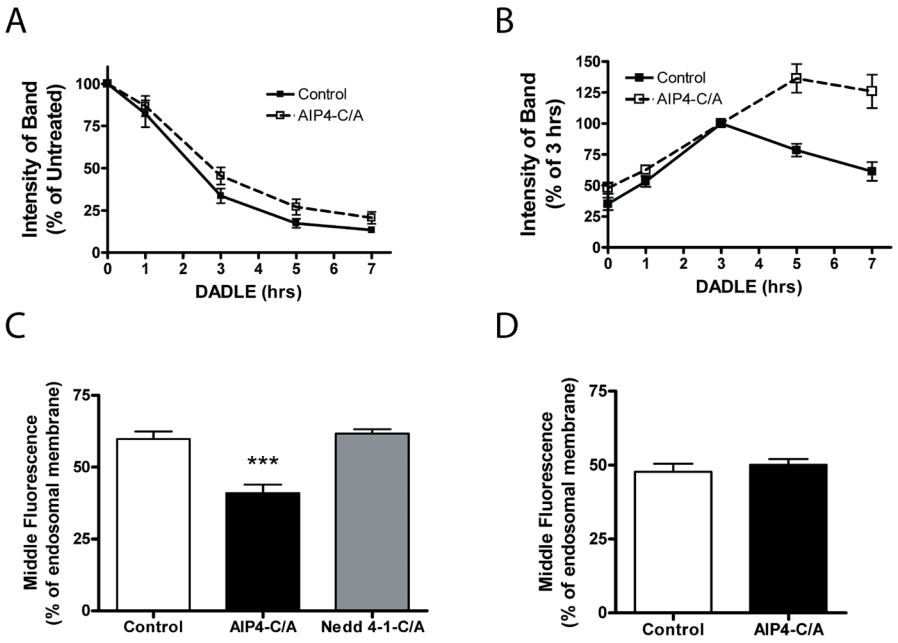

Figure 8. The E3 ubiquitin ligase AIP4 regulates transfer of DORs to ILVs and subsequent C-terminal proteolysis of receptors

A and B) HEK293 cells stably expressing F-DOR-HA were transfected with either control plasmid (pcDNA) or one expressing mycAIP4-C/A. Cells were then incubated with 10μM DADLE for the indicated time period before lysis and division into two identical samples. Blots generated across multiple experiments were scanned and densitometry performed to estimate the amount of FLAG-tagged receptors remaining at each time point relative to agonist naïve cells (**A**), and the relative abundance of one anti-HA immunoreactive proteolytic product expressed as a percentage of density at 3 hrs agonist treatment (**B**). Shown are the mean and SEM of multiple experiments (n=6); closed symbols indicate results from control-transfected cells, and open symbols from cells expressing mycAIP4-C/A. **C)** HEK 293 cells were transfected with F-DOR-GFP and mCherry-AIP4-C/A or mCherry-Nedd4-1-C/A, replated onto coverslips, and incubated for 90 min with 10μM DADLE before imaging. Quantification of the middle fluorescence measured from individual endosomes is shown. Mean and SEM of middle fluorescence values are shown for F-DOR-GFP transfected cells (Control, n= 12 cells, 50 endosomes), F-DOR-GFP and mCherry AIP4-C/A transfected cells (AIP4-C/A, unpaired t-test; ***, $p<0.0001$, n= 16 cells, 51 endosomes), and F-DOR-GFP and mCherry-Nedd 4-1-C/A transfected cells (Nedd4-1-C/A, n= 10 cells, 82 endosomes). **D)** HEK 293 cells were transfected with F-DOR0cK-GFP and mCherry-AIP4-C/A, replated onto coverslips, and incubated for 90 min with 10μM DADLE before imaging. the quantification of the mean middle fluorescence, measured from individual endosomes of Control (n= 14 cells, 59 endosomes) and AIP4-C/A (n= 11 cells, 53 endosomes) is shown.

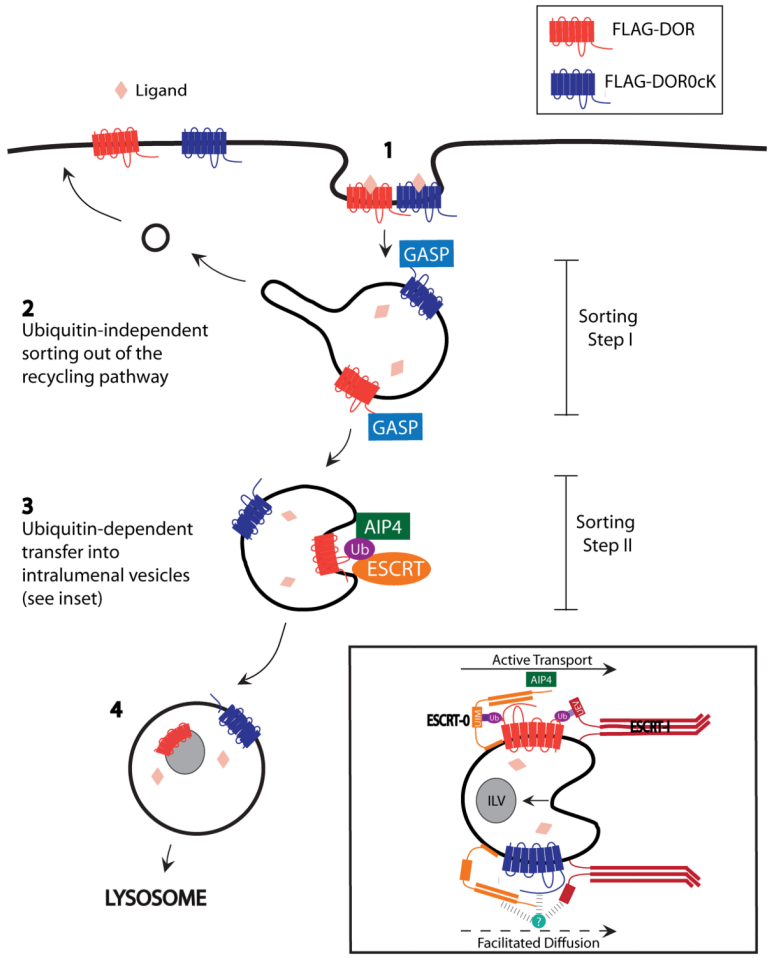

Figure 9. Model for sequential ubiquitin-independent –and dependent regulation of DOR degradation

The wild type DOR, as well as the lysine mutant DOR0cK that cannot be ubiquitinated, undergo regulated endocytosis following ligand-induced activation (1). Receptors are prevented from traversing the default recycling pathway by 'Sorting step I', which does not require receptor ubiquitination and is sensitive to ubiquitination-independent interaction of receptors with GASPs (2). Receptors undergo topological sorting from the limiting membrane to ILVs; this represents a discrete operation that we call 'Sorting step II'. Sorting step II resembles canonical ubiquitin-dependent sorting of other cargo and requires the ESCRT. The difference is that DORs can still undergo transfer to ILVs, albeit with moderately reduced rate or efficiency, when receptor ubiquitination is prevented (3). This sequential organization of discrete sorting operations, together with (partial) ubiquitination-dependence specifically of the downstream step, explains the ability of lysine-mutant DORs to down-regulate effectively via the canonical pathway. Accordingly, lysine mutation causes a selective and partial inhibition of later proteolytic events that require protease access to the receptor's cytoplasmic surface (4).